CHEMISTRY OF MATERIALS
Article

Chem. Mater. **2010,** *22,* 6103–6108 6103
DOI:10.1021/cm1015965

Colloidal Synthesis of Air-Stable Crystalline Germanium Nanoparticles with Tunable Sizes and Shapes

Dimitri D. Vaughn II, James F. Bondi, and Raymond E. Schaak*

Department of Chemistry and Materials Research Institute, The Pennsylvania State University, University Park, Pennsylvania 16802, United States

Received June 8, 2010. Revised Manuscript Received October 3, 2010

Nanoparticles of elemental germanium have interesting optical and electronic properties and relatively low toxicity, making them attractive materials for biological and optoelectronic applications. The most common routes to colloidal Ge nanoparticles include metathesis reactions involving Zintl salts, hydride reduction of Ge halides, and thermal decomposition of organogermane precursors. Here we describe an alternative "heat-up" method for the synthesis of size- and shape-tunable Ge nanoparticles that are both crystalline and air stable. The readily available reagents GeI_4, oleylamine, oleic acid, and hexamethyldisilazane are combined in one pot and heated to 260 °C, where a rapid nucleation event occurs and multifaceted nanoparticles of crystalline Ge form. By varying the concentration of GeI_4, the nanoparticle size can be tuned from 6 to 22 nm with narrow size distributions. Adding trioctylphosphine yields cube-shaped particles, and switching the solvent to octadecene yields one-dimensional nanostructures. The Ge nanoparticles, which are fully air stable for more than 6 months, were characterized by XRD, TEM, HRTEM, EDS, XPS, DRIFT, and UV−visible spectroscopy.

Introduction

Germanium nanoparticles (Ge NPs) are an important target for colloidal synthesis. Elemental Ge has important applications in many optoelectronic devices that include photodetectors,[1−3] field-effect transistors,[4,5] and multijunction solar cells.[6,7] Because of the low cost and relative ease of solution-based processing techniques such as spin coating, dip coating, and inkjet printing, colloidally stable solutions of Ge nanoparticles could be useful materials for the cost-effective fabrication of these and related devices.[8,9] Furthermore, Ge NPs have low toxicity and have been shown to exhibit size-dependent photoluminescence (PL) properties,[10,11] suggesting potential biological applications that include cell imaging, labeling, and photothermal therapy.[12] Finally, given the ability of elemental nanoparticles to serve as reactive templates for chemical transformation into derivative nanostructures,[13] colloidal Ge NPs could serve as precursors to related Ge-based systems, including thermoelectric alloys,[14,15] phase change materials,[16] and narrow band gap semiconductors.[17−19]

Synthetic capabilities for size- and shape-tunable colloidal Ge NPs remain less developed than those for the ubiquitous II−VI, III−V, and IV−VI semiconductor nanocrystals, such as CdSe, InAs, ZnS, etc.[20−23] To synthesize Ge NPs using colloidal methods, three general strategies have been predominant in the literature: metathesis reactions involving Zintl salts,[24−28] hydride reduction

*Corresponding author. E-mail: schaak@chem.psu.edu.

(1) Michel, J.; Liu, J.; Kimerling, L. C. *Nat. Photonics* **2010**, *4*, 527.
(2) Assefa, S.; Xia, F.; Vlasov, Y. A. *Nature* **2010**, *464*, 80.
(3) Yan, C.; Singh, N.; Cai, H.; Gan, C. L.; Lee, P. S. *ACS Appl. Mater. Interfaces* **2010**, *2*, 1794.
(4) Kamata, Y. *Mater. Today* **2008**, *11*, 30.
(5) Wu, X.; Kulkarni, J. S.; Collins, G.; Petkov, N.; Almecija, D.; Boland, J. J.; Erts, D.; Holmes, J. D. *Chem. Mater.* **2008**, *20*, 5954.
(6) Guter, W.; Schone, J.; Philipps, S. P.; Steiner, M.; Siefer, G.; Wekkeli, A.; Welser, E.; Oliva, E.; Bett, A. W.; Dimroth, F. *Appl. Phys. Lett.* **2009**, *94*, 223504.
(7) Law, D. C.; King, R. R.; Yoon, H.; Archer, M. J.; Boca, A.; Fetzer, C. M.; Mesropian, S.; Isshiki, T.; Haddad, M.; Edmondson, K. M.; Bhusari, D.; Yen, J.; Sherif, R. A.; Atwater, H. A.; Karam, N. H. *Sol. Energ. Mat. Sol. C.* **2008**, *94*, 1314.
(8) Sargent, E. H. *Nat. Photonics* **2009**, *3*, 332.
(9) Talapin, D. V.; Lee, J. S.; Kovalenko, M. V.; Shevchenko, E. V. *Chem. Rev.* **2010**, *110*, 389.
(10) Heath, J. R.; Shiang, J. J.; Alivisatos, A. P. *J. Chem. Phys.* **1994**, *101*, 1607.
(11) Wilcoxon, J. P.; Provencio, P. P.; Samara, G. A. *Phys. Rev. B* **2001**, *64*, 035417.
(12) Fan, J.; Chu, P. K. *Small* **2010**, *6*, 2080.
(13) Vasquez, Y.; Henkes, A. E.; Bauer, J. C.; Schaak, R. E. *J. Solid State Chem.* **2008**, *181*, 1509.
(14) Tsybeskov, L.; Lockwood, D. J. *Proc. IEEE* **2009**, *97*, 1284.
(15) Lan, Y.; Minnich, A. J.; Chen, G.; Ren, Z. *Adv. Funct. Mater.* **2010**, *20*, 357.
(16) Raoux, S.; Welnic, W.; Ielmini, D. *Chem. Rev.* **2010**, *110*, 240.
(17) Yoon, S. M.; Song, H. J.; Choi, H. C. *Adv. Mater.* **2010**, *22*, 2164.
(18) Makinistian, L.; Albanesi, E. A. *J. Phys.: Condens. Matter* **2007**, *19*, 186211.
(19) Makinistian, L.; Albanesi, E. A. *Phys. Rev. B* **2006**, *74*, 045206.
(20) Yin, Y.; Alivisatos, A. P. *Nature* **2005**, *437*, 664.
(21) Kumar, S.; Nann, T. *Small* **2006**, *2*, 316.
(22) Murray, C. B.; Kagan, C. R.; Bawendi, M. G. *Annu. Rev. Mater. Sci.* **2000**, *30*, 545.
(23) Guzelian, A. A.; Banin, U.; Kadavanich, A. V.; Peng, X.; Alivisatos, A. P. *Appl. Phys. Lett.* **1996**, *69*, 1432.
(24) Taylor, B. R.; Kauzlarich, S. M.; Delgado, G. R.; Lee, H. W. H. *Chem. Mater.* **1999**, *11*, 2493.
(25) Ma, X.; Wu, F.; Kauzlarich, S. M. *J. Solid State Chem.* **2008**, *181*, 1628.
(26) Chiu, H. W.; Kauzlarich, S. M. *Chem. Mater.* **2006**, *18*, 1023.
(27) Hope-Weeks, L. J. *Chem. Commun.* **2003**, 2980.
(28) Wang, W. Z.; Poudel, B.; Huang, J. Y.; Wang, D. Z.; Kunwar, S.; Ren, Z. F. *Nanotechnology* **2005**, *16*, 1126.

Published on Web 11/01/2010

of germanium halides,[29−34] and thermal decomposition of organogermane precursors in high boiling point solvents.[35−39] While these methods have had some success at generating crystalline Ge NPs with some degree of size and/or morphology control, there are key aspects that remain to be improved. The covalent nature of Ge leads to high crystallization temperatures that are often above the boiling points of commonly used solvents. As a result, several of the reported solution routes to Ge NPs yield amorphous products that are often unstable relative to dissolution and oxidation.[26,30,32,36] To overcome this, highly reactive reducing agents (e.g., Na, $LiAlH_4$, n-BuLi) have been essential for the production of crystalline Ge NPs.[24,29,40] However, these methods are not optimal from an ease-of-synthesis perspective, and they can also form toxic byproducts.[41] Therefore, a simpler and milder approach for synthesizing crystalline and air-stable colloidal Ge NPs with tunable sizes and shapes would help to further advance the applicability of these materials.

Here, we report an alternative route to crystalline Ge nanoparticles, which is inspired by the "heat-up" method that has been used successfully in the synthesis of metal, metal oxide, and chalcogenide nanocrystals.[42,43] In this approach, all precursors are dissolved in a reducing solvent at room temperature and slowly heated in a one-pot system to facilitate reduction, supersaturation, and nucleation that results in the formation of nanoparticles. The reagents used to generate Ge NPs are GeI_4, oleylamine, oleic acid, and hexamethyldisilazane (HMDS), which are all air-stable and commercially available. After heating to 260 °C, Ge NPs nucleate rapidly, and their average sizes can be tuned from 6−22 nm by varying the concentration of GeI_4. Changing the solvent and varying the surfactant concentrations can also access different morphologies of Ge NPs including cube-shaped and one-dimensional nanostructures. In addition, the Ge NPs are air-stable for several months, with no evidence of oxidative degradation.

(29) Prabakar, S.; Shiohara, A.; Hanada, S.; Fujioka, K.; Yamamoto, K.; Tilley, R. D. *Chem. Mater.* **2010**, *22*, 482.
(30) Chou, N. H.; Oyler, K. D.; Motl, N. E.; Schaak, R. E. *Chem. Mater.* **2009**, *21*, 4105.
(31) Warner, J. H.; Tilley, R. D. *Nanotechnology* **2006**, *17*, 3745.
(32) Lu, X.; Korgel, B. A.; Johnston, K. P. *Chem. Mater.* **2005**, *17*, 6479.
(33) Wu, H. P.; Liu, J. F.; Wang, Y. W.; Zeng, Y. W.; Jiang, J. Z. *Mater. Lett.* **2006**, *60*, 986.
(34) Fok, E.; Shih, M.; Meldrum, A.; Veinot, J. G. C. *Chem. Commun.* **2004**, 386.
(35) Wang, Y. W.; Zeng, Y. W.; Wang, L. N.; Zhang, G. Q.; Jiang, J. Z. *Nanotechnology* **2006**, *17*, 5339.
(36) Zaitseva, N.; Dai, Z. R.; Grant, C. D.; Harper, J.; Saw, C. *Chem. Mater.* **2007**, *19*, 5174.
(37) Warner, J. H. *Nanotechnology* **2006**, *17*, 5613.
(38) Gerung, H.; Bunge, S. D.; Boyle, T. J.; Brinker, C. J.; Han, S. M. *Chem. Commun.* **2005**, *14*, 1914.
(39) Gerion, D.; Zaitseva, N.; Saw, C.; Casula, M. F.; Fakra, S.; Buuren, T. V.; Galli, G. *Nano Lett.* **2004**, *4*, 597.
(40) Lee, D. C.; Pietryga, J. M.; Robel, I.; Werder, D. J.; Schaller, R. D.; Klimov, V. I. *J. Am. Chem. Soc.* **2009**, *131*, 3436.
(41) Wilcoxon, J. P.; Provencio, P. P.; Samara, G. A. *Phys. Rev. B* **2007**, *76*, 199904.
(42) Kwon, S. G.; Hyeon, T. *Acc. Chem. Res.* **2008**, *41*, 1696.
(43) Park, J.; Joo, J.; Kwon, S. G.; Jang, Y.; Hyeon, T. *Angew. Chem., Int. Ed.* **2007**, *46*, 4630.

Experimental Section

Materials. Oleylamine, oleic acid, 1-octadecene, and tri-n-octylphosphine were degassed prior to use. All other chemicals were used as received. Germanium(IV) iodide (GeI_4, 99.99+%), tri-*n*-octylphosphine (TOP, 90% tech.), oleylamine (70% tech.) and hexamethyldisilazane (HMDS, >99%) were purchased from Aldrich. Oleic acid (90% tech.), 1-octadecence (90% tech.), biphenyl-4-carboxylic acid (98%), and *p*-toluenesulfonic acid (99%) were purchased from Alfa Aesar. All syntheses were carried out under Ar using standard Schlenk techniques, and purification procedures were performed in air.

Synthesis. Multifaceted Ge nanocrystals were synthesized by first loading a 20 mL scintillation vial with 60 mg (0.10 mmol) of GeI_4 and adding 10 mL (~30 mmol) of oleylamine and 0.75 mL (2.38 mmol) of oleic acid. The solution was sonicated for ~5 min to give a clear colorless solution, which was then inserted into a 3-neck round-bottom flask fitted with condenser, thermometer, and rubber septum. Next, 1 mL (4.71 mmol) of HMDS was added to the mixture and the solution was slowly heated (~2 °C/min) to 260 °C. During the heating process, the solution changed from colorless to yellow and at 260 °C changed from yellow to a dark brown-red almost instantaneously. This solution was aged for a maximum of 30 min.

Cube-shaped Ge nanoparticles were synthesized in a similar manner, except that 0.5 mL (1.12 mmol) of tri-*n*-octylphosphine was added as a cosurfactant and 0.5 mL (1.59 mmol) of oleic acid was used. Oleylamine and hexamethyldisilazane were held at their same concentrations. During the heating process, the solution changed from colorless to yellow to brown (260 °C) and finally to a deep purple (within a few minutes). This reaction also resulted in rapid nucleation at 260 °C and was aged for a maximum of 30 min. One-dimensional Ge nanostructures were synthesized by using a 12:1 ratio of oleylamine to GeI_4: 60 mg (0.10 mmol) of GeI_4, 400 μL (1.21 mmol) of oleylamine, 5 mL (~16 mmol) of 1-octadecene, and 1 mL of HMDS. The synthetic details were identical, except that the solution was rapidly heated to the reflux temperature of 1-octadecene (315 °C). During heating, the solution changed from orange to colorless to yellow and at 260 °C became a light orange color. The reaction was aged overnight at reflux, which resulted in the formation of a light purple solution.

To purify all Ge nanostructures, we first precipitated the products by adding 30 mL of 100% ethanol and then centrifuged them at 12 000 rpm for 10 min. The obtained powders were then washed three times with a 1:1 toluene:ethanol mixture with centrifugation between each wash. The products could be suspended in toluene or hexanes for further characterization.

Characterization. Powder X-ray diffraction (XRD) data were collected using a Bruker D8 Advance X-ray diffractometer equipped with CuKα radiation. UV−visible absorption spectra were collected in toluene solution at room temperature in 1 cm quartz cuvettes using an Ocean Optics DH-2000-BAL spectrometer. Transmission electron microscopy (TEM) images and selected area electron diffraction (SAED) patterns were obtained using a JEOL 1200 EX II operating at 80 kV. High resolution transmission electron microscopy (HRTEM) imaging and energy-dispersive spectroscopy (EDS) analyses were performed on a JEOL-2010 LaB_6 microscope operating at 200 kV. TEM samples were prepared by suspending the washed crystallites in toluene and drop-casting onto Formvar-coated copper TEM grids. Data for size distribution histograms was acquired by measuring the longest dimension of each nanoparticle for more than 100 particles per sample. X-ray photoelectron spectroscopy (XPS) was performed on a monochromatic Al Kα

source instrument (Kratos, Axis Ultra, England) operating at 14 kV and 20 mA for an X-ray power of 280 W. XPS spectra were collected with a photoelectron take off angle of 90° from the sample surface plane, energy steps of 0.20 eV, and a pass energy of 20 eV. All XPS spectra were referenced to the C 1s peak with a binding energy of 284.5 eV. Infrared spectra were acquired on an IFS 66/s spectrometer (Bruker Optics, Billerica, MA) using a Collector II diffuse reflection accessory equipped with a high temperature/vacuum (HTV) sample chamber (Thermo Spectra-Tech, Madison, WI). The HTV cell was outfitted with KBr windows (New Era Enterprises, Vineland, NJ) and operated under purge with UHP Argon (Grade 5.0, PraxAir). Spectra were acquired at ~30 °C after briefly heating to ~100 °C to facilitate the removal of adsorbed water and minimize the interference of the OH deformation band of water at ~1640 cm^{-1}.

Results and Discussion

Synthesis and Characterization of Multifaceted Ge Nanoparticles. Figure 1a and Figure S1 in the Supporting Information show a large-area TEM image for a representative sample of Ge nanoparticles produced by slowly heating a mixture of GeI_4, oleylamine, oleic acid, and HMDS to 260 °C for 30 min. The SAED pattern in Figure 1b indicates the presence of crystalline Ge with no other observable crystalline impurities. The HRTEM image in the inset to Figure 1a confirms that the Ge particles are largely single-crystalline with observable lattice fringes corresponding to the (111) plane of diamond-type Ge. A higher-magnification TEM image of this sample is shown in Figure 2a, along with the size distribution histogram that indicates an average size of 22 ± 4 nm. The shape of the particles is nominally isotropic with irregular facets, but the average size is fairly uniform.

By decreasing the initial concentration of GeI_4 while keeping all other conditions and concentrations unchanged, the average sizes of the Ge NPs could be tuned to below the Bohr radius of Ge (R_b = 11.5 nm).[29] For example, the 22 ± 4 nm particles shown in Figures 1 and 2a formed when 60 mg of GeI_4 was used. When the amount of GeI_4 decreased to 30 mg, the particles appeared morphologically similar but with a smaller average size, 12 ± 2 nm. In addition, a small (< 5%) population of irregular 1−2 nm particles is observed in some samples, but because of the difficulty in accurately measuring their sizes, these were not included in the histogram shown in Figure 2b. When the amount of GeI_4 was further decreased to 15 mg, the average size of the particles decreased to 6 ± 1 nm. The SAED patterns in Figure 2 confirm the formation of Ge nanoparticles in each case.

Figure 3 shows powder XRD patterns for each of the samples in Figure 2. The XRD data indicate that all of the samples correspond to crystalline Ge with no observable crystalline impurities. This agrees well with the SAED patterns in Figures 1 and 2. Scherrer analysis of the (111) peak widths estimates average grain sizes of 17, 11, and 8 nm for the samples shown in Figure 2a−c, respectively. These values are consistent with the particle sizes observed by TEM, within experimental error. This agreement suggests that the particles are predominantly single crystals, which is validated by the HRTEM image in Figure 1a. UV−visible absorption spectra for the Ge NPs (see Figure S2 in the Supporting Information) show a continuous red shift in absorption from approximately 450 to 490 nm as the particle size increases from 6 to 22 nm. This is consistent with previous reports of UV−vis absorption spectra for quantum-confined Ge nanoparticles.[37,38] A photoluminescence response was not observed in the UV−visible region.[40]

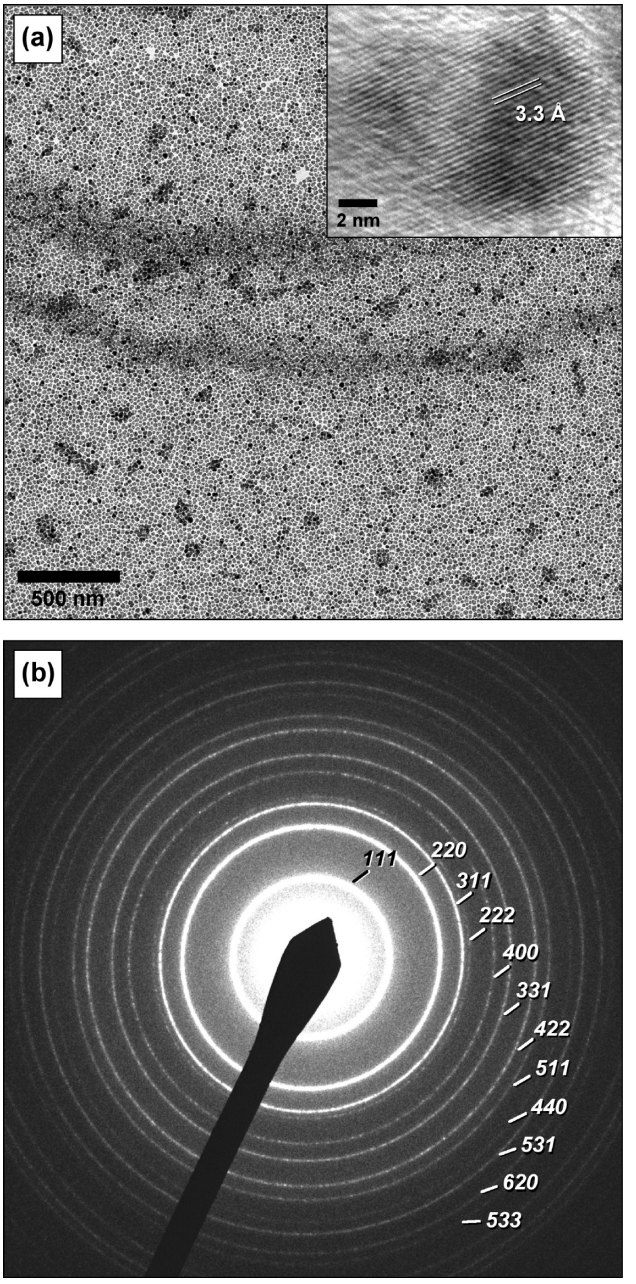

Figure 1. Representative (a) large-area TEM image and (b) SAED pattern for crystalline Ge nanoparticles. A representative HRTEM image, showing lattice fringes corresponding to the (111) plane of diamond-type Ge, is shown in the inset to image a.

Using this synthetic method, crystalline Ge nanoparticles form following a rapid nucleation event around 260 °C. A series of control experiments help to uncover the key variables that are critical for the formation of crystalline Ge nanoparticles. First, HMDS is required; control experiments without HMDS produced only an amorphous

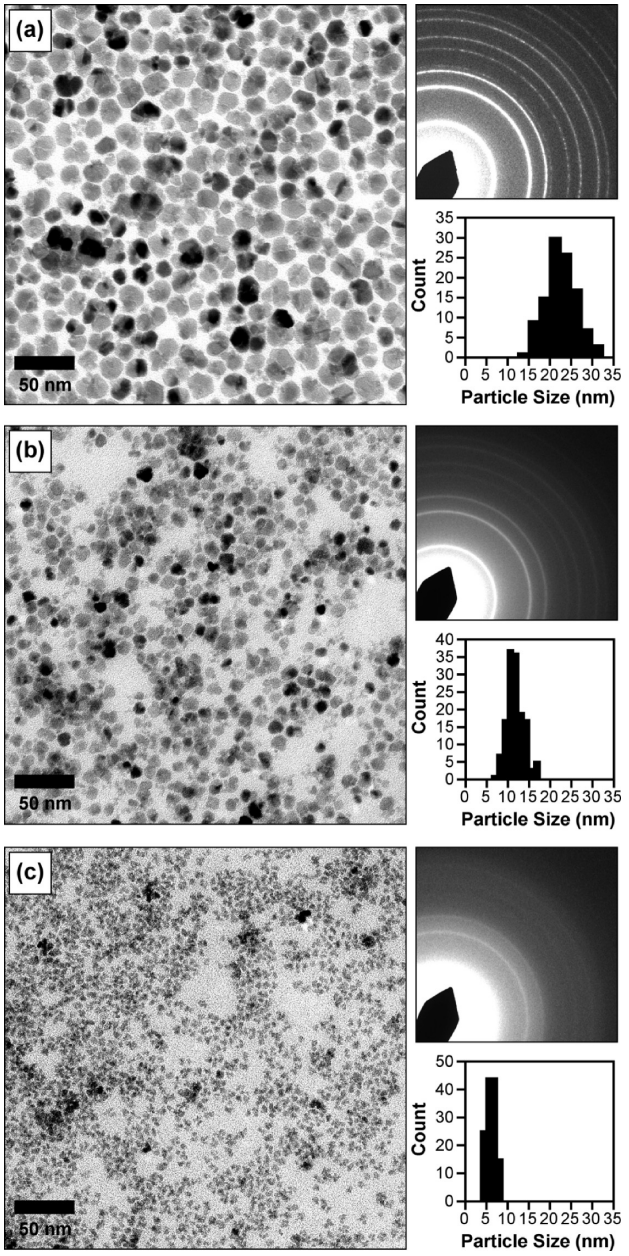

Figure 2. TEM images, SAED patterns, and size distribution histograms for Ge nanoparticles with average sizes of (a) 22 ± 4 nm (same sample shown in Figure 1), (b) 12 ± 2 nm, and (c) 6 ± 1 nm.

product that was highly susceptible to oxidation. Boyle and co-workers[38] previously produced crystalline Ge nanoparticles via the thermal decomposition of a Ge(II)-HMDS complex, $Ge[N(SiMe_3)_2]_2$, that was synthesized and purified as part of a multistep reaction, so a Ge-HMDS complex may play a role in the formation of Ge NPs in our system as well. In addition, the presence of an organic acid (e.g., oleic acid) in an optimal 1:2 ratio with HMDS was necessary to form nonaggregated particles. With no organic acid present, crystalline Ge does not form until above 320 °C and the particles are highly agglomerated (see Figure S3 in the Supporting Information). Replacing oleic acid with other organic acids, such as biphenyl-4-carboxylic acid and *p*-toluenesulfonic acid, yielded results similar to those observed with oleic acid.

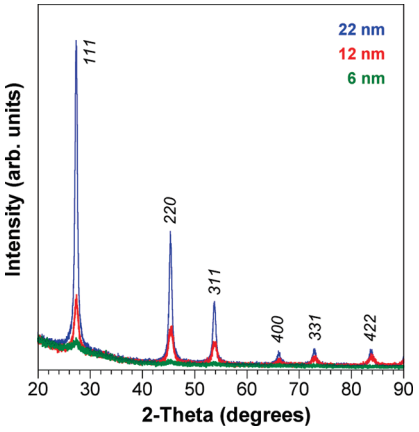

Figure 3. Powder XRD patterns for Ge nanoparticles with average sizes of 22 nm (blue), 16 nm (red), and 6 nm (green).

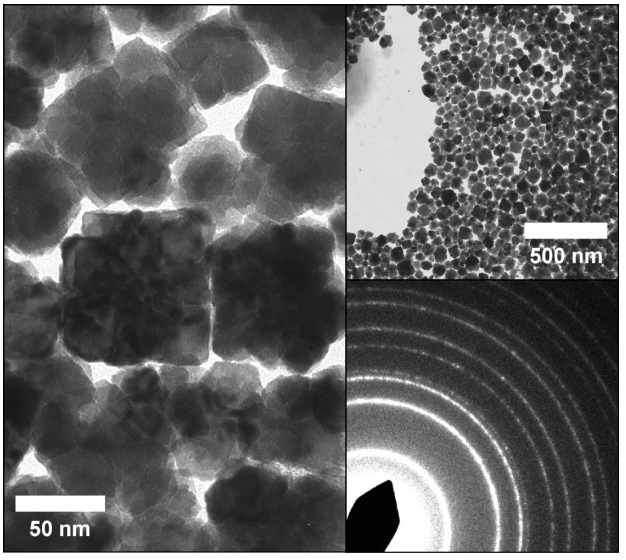

Figure 4. TEM images and SAED pattern for cube-shaped Ge nanoparticles synthesized using a TOP/oleylamine mixture.

Cube-Shaped Nanoparticles and One-Dimensional Nanostructures. Once the key parameters for generating crystalline Ge were identified (the presence of HMDS and organic acids), other variables were studied in order to change the morphology. Adding TOP in a 2:3 ratio with oleic acid while all other concentrations remained constant generated crystalline Ge nanoparticles via the same rapid nucleation event at 260 °C. However, instead of the multifaceted nanocrystals observed without TOP (Figures 1 and 2), cube-shaped particles were predominant. The TEM images in Figure 4 show particles with an average edge length of 73 ± 16 nm. The SAED pattern confirms that the cube-shaped particles correspond to crystalline Ge. Particles with cube-like morphologies, e.g., those that have predominantly flat edges, represent approximately 60% of the sample based on analysis of multiple TEM images.

When the solvent is changed from oleylamine to octadecene with only a stoichiometric amount of oleylamine present (12:1 oleylamine: GeI_4), one-dimensional nanostructures form (Figure 5a,b,d). The SAED pattern in Figure 5c confirms that the one-dimensional nanostructures are composed of crystalline diamond-type Ge and

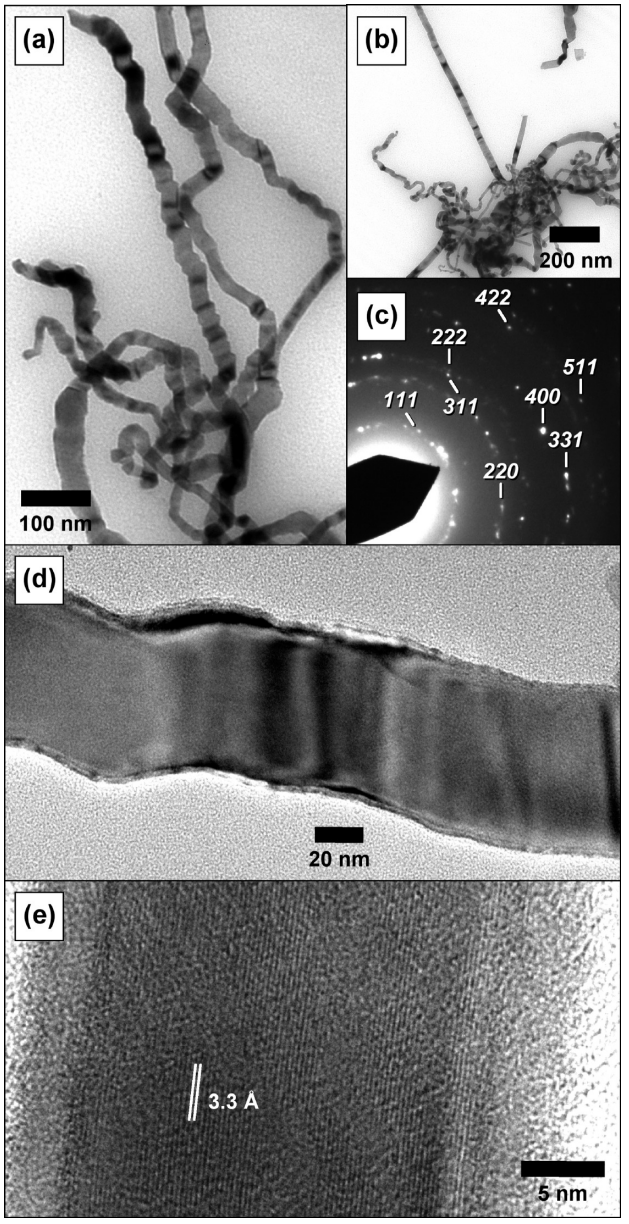

Figure 5. (a, b) TEM images, (c) SAED pattern, and (d, e) HRTEM images for one-dimensional Ge nanostructures synthesized using octadecene as the solvent. Panel (e) shows lattice fringes corresponding to the (111) plane of diamond-type Ge.

EDS spectra indicate the presence of only Ge (see Figure S4 in the Supporting Information). The HRTEM image in Figure 5e confirms that the one-dimensional nanostructures are crystalline, and lattice fringes corresponding to the (111) planes of diamond-type Ge are observed. The formation of a thin amorphous layer on the surface of the one-dimensional Ge nanostructures is also evident, and this is likely attributable to amorphous GeO_2.

Surface and Stability. The Ge nanoparticles synthesized using this one-pot protocol appear to be air-stable for long periods of time. Figure 6 shows a powder XRD pattern for a representative sample of Ge nanoparticles as-synthesized, as well as an XRD pattern for the same sample acquired six months later after storage in powder form under ambient conditions. The two patterns are fully superimposable with no evidence of degradation or

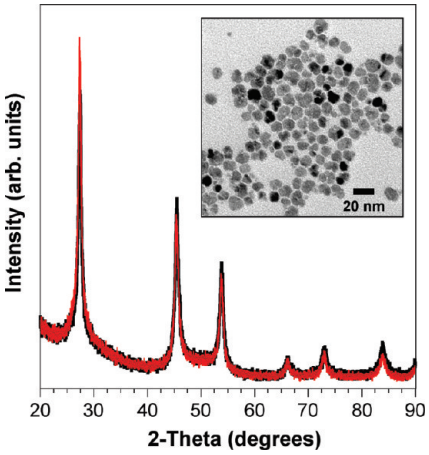

Figure 6. Powder XRD patterns for a representative sample of crystalline Ge nanoparticles as-synthesized (black) and after six months of storage in powder form under ambient conditions (red). Inset: TEM image of the Ge nanoparticle sample from Figure 1 after more than 6 months of storage under ambient conditions.

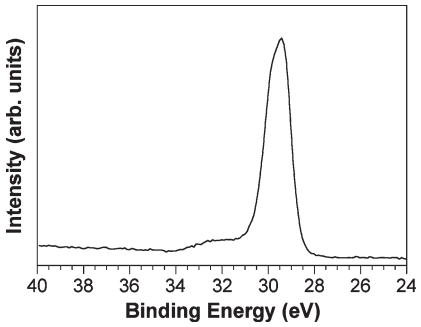

Figure 7. Representative XPS spectrum (3d core region) for the Ge nanoparticles shown in Figure 1.

oxidation, demonstrating that they are highly air-stable with surfaces that are apparently well-passivated. A TEM image of the particles from Figure 1, after being stored in air for six months, is shown in the inset to Figure 6. The morphology remains the same, even after many months of ambient storage, with no evidence of degradation.

Figure 7 shows an XPS spectrum for the 3d core region of a representative sample of as-synthesized Ge NPs after more than 6 months of aging (in powder form) under ambient conditions. Deconvolution of the XPS data indicates 86% Ge^0, with a binding energy of 29.4 eV,[32] and 14% Ge^{4+}, with a binding energy between 32 and 33 eV. Similar ratios of Ge^0 to Ge^{4+} were found in the as-synthesized sample. This indicates that a majority of the Ge is zerovalent, with only a small amount of oxidized Ge, both as-synthesized and after 6 months of ambient storage.

Analysis by diffuse reflectance infrared Fourier transform (DRIFT) spectroscopy indicated a cis C−H alkene stretch at ~3010 cm^{-1} (see Figure S5 in the Supporting Information) and C=O stretching modes appearing as minor shoulders at ~1685 and 1510 cm^{-1}.[44] This is consistent with the presence of oleic acid on the Ge surface, although we cannot rule out the possibility that other

(44) Lee, D. H.; Condrate, R. A. *J. Mater. Sci.* **1999**, *34*, 139.

organic species may also be present. Taken together, the data (XPS, DRIFT, and HRTEM) suggest that a thin layer of amorphous germanium oxide, to which oleate groups are bound, caps the elemental Ge nanoparticles. A similar passivation scheme was suggested for colloidally synthesized elemental Mn nanoparticles, which were also highly air stable.[45]

Conclusions

In summary, we have described a simple one-pot route to colloidal Ge nanoparticles that is based upon the "heat up" method. The as-synthesized particles are highly crystalline and stable relative to oxidation and chemical degradation. This synthesis uses chemical reagents that are readily available and air stable (GeI_4, oleylamine, oleic acid, and HMDS), providing an approach for the synthesis of crystalline Ge nanoparticles that is milder than most existing methods. Simply changing the concentration of GeI_4 can access nanoparticles with average sizes that are tunable from approximately 6 to 22 nm, and additional modifications (e.g., other solvents or stabilizer mixtures) can lead to shapes that include cube-shaped nanoparticles and one-dimensional nanostructures. In analogy to other colloidal semiconductor nanoparticles made using related methods,[21,42] modifications to this approach may lead to different morphologies.

Acknowledgment. This work was primarily supported by the U.S. Department of Energy, Office of Basic Energy Sciences, Division of Materials Sciences and Engineering, under Award #DE-FG02-08ER46483 (R.E.S., J.F.B., materials synthesis and characterization). D.D.V acknowledges partial support from the Penn State MRSEC (DMR-0820404), the Bunton-Waller Fellows Program, and an NSF Graduate Research Fellowship. TEM imaging was performed in the Electron Microscopy Facility of the Huck Institutes of the Life Sciences and in the Materials Characterization Facility at the Penn State Materials Research Institute. The authors acknowledge use of facilities at the PSU site of the NSF NNIN. The authors also thank Josh Stapleton for acquisition of the DRIFT data and Tad Daniels for acquiring the XPS data.

Supporting Information Available: UV−vis, EDS, and DRIFT spectra, as well as additional TEM images. This material is available free of charge via the Internet at http://pubs.acs.org.

(45) Bondi, J. F.; Oyler, K. D.; Ke, X.; Schiffer, P.; Schaak, R. E. *J. Am. Chem. Soc.* **2009**, *131*, 9144.